ELSEVIER
Comput. Methods Appl. Mech. Engrg. 173 (1999) 201–215
Computer methods in applied mechanics and engineering

On an adaptive monotonic convection–diffusion flux discretization scheme

Tony W.H. Sheu[a,*], C.C. Fang[a], S.F. Tsai[a], Chung-Yuan Huang[b]

[a]*Department of Naval Architecture and Ocean Engineering, National Taiwan University, 73 Chou-Shan Rd., Taipei, Taiwan, Republic of China*

[b]*Department of Mechanical Engineering, National Taiwan Institute of Technology, Taipei, Taiwan, Republic of China*

Abstract

The present paper concerns numerical investigation of a two-dimensional steady convection–diffusion scalar equation. Specific attention is given to resolving spurious oscillations in a confined region of high gradient. In smooth regions, a high-order accurate solution is desired, while in regions containing a sharp gradient, the strategy of applying a monotonic capturing scheme is preferred. In this paper, we model fluxes by means of a finite element model which has spaces spanned by Legendre polynomials. The propensity to yield an irreducible diagonal-dominant stiffness matrix is an attribute of this finite element flux discretization scheme. Fundamental analyses are extensively conducted in this paper in two areas. First, by conducting a modified equation analysis, we are led to confirm the consistency of the scheme. Both the stability and monotonicity of the solutions are also addressed. A guide for judging whether the stiffness matrix can yield a monotonic solution is rooted in the theory of the *M*-matrix. This monotonicity study provides us with greater numerical insight into the importance of the chosen Peclet number. Beyond its critical value, oscillatory solutions are present in the flow. This monotonic region is, however, fairly restricted. It is this shortcoming which limits the finite element practioner's choices for fairly small grid size. The scope of application using the proposed upwind scheme is, thus, rather small because monotonic solutions are prohibitively expensive to compute. Circumvention of such deficiency is accomplished by making modifications to the structured grid. Several test cases have been employed to examine the grid adaption technique for the treatment of advection terms in flow regions having sharp gradients. Considerable savings in computer storage and execution time are achieved by the employed unstructured grid setting.

1. Introduction

The incompressible viscous flow, among others, has, in the past, received considerable attention since this flow is relevant to many industrial applications. Bearing in mind that the scalar convection–diffusion equation is the simplest prototype for this class of flow, better understanding of this passive transport equation is a subject of fundamental importance in fluid mechanics and has been the focus of intensive study for many years. Working equations of this type are also of considerable engineering interest because they are amenable to analytic solution, and thus provides a convenient test for detailed assessment of the discretization methods so far devised. It is for this reason that this model problem is the continuous subject of much research interest, academically as well as practically. Over the past 40 years, computers have increased in speed roughly by an order of magnitude per decade. Parallel to hardware developments, computational methods have played an ever-increasing role in the design of new industrial products. After many years of research, however, the solution of the multi-dimensional scalar convection–diffusion equation, for example, still remains an open question. Some progress has been made, but answers are not definite yet. More work needs to be done in this area to achieve 'robust' results, and this was the motivation for the present study.

* Corresponding author. Fax: 886-2-23929885; e-mail: sheu@indy.na.ntu.edu.tw

0045-7825/99/$ – see front matter
PII: S0045-7825(98)00269-2

In numerical modeling of a convection–diffusion transport equation, numerical dissipation and numerical dispersion, or numerical diffusion as a whole, are the major causes of numerical spreading. Numerical dissipation refers to artificially introduced smearing of the predicted profile while numerical dispersion refers to non-physical spatial oscillations in the solution. A guide for assessing simulation quality is constructed on the basis of solution accuracy, numerical stability, computational efficiency, scheme consistency and ease of programming. Achieving all these desired properties is very difficult. What fits for solution accuracy may not for solution stability. For instance, use of a full doner cell upwind scheme enhances the stability of the discrete system. For flow conditions classified as having high Peclet numbers, there is, however, gross smearing of the solution due to excessive addition of artificial viscosities. The stable numerical results thus obtained will probably be unacceptable because the real transport phenomenon has been contaminated by large errors introduced in the upwinding procedure. For a flow at an angle to the grid, false diffusion errors further deteriorate the solution quality by gross distortion of the advective profile.

Various discretization schemes for alleviating false diffusion errors have been proposed and evaluated. In many flows, steep gradients appear, complicating further the development of flux discretization. In these circumstances, a flow-oriented flux discretization scheme no longer suffices for production of oscillation-free solutions. Difficulties in suppressing over- or undershoots in the solution have led to the development of bounding schemes. Much of the previous work has been devoted to one-dimensional analysis. The distinguishing feature of this work is the accommodation of the total variational diminishing (TVD) property [1]. However, we are still faced with the task of bringing this desirable monotonic property into multi-dimensional schemes. The flux corrected transport (FCT) algorithm of Boris and Book [2], which was later generalized by Zalesak [3], is regarded as the first multi-dimensional high-resolution scheme developed by the finite difference/volume community. This scheme, together with the Filter Remedy and Methodology (FARM) of Chapman [4] and several variants of flux limiters, has been applied to simulation of different classes of equations by one of the present authors [5,6]. Among other schemes, a simple High-Accuracy Resolution Program (SHARP) [7] and Nonoscillatory Integrally Reconstructed Volume-Averaged Numerical Advection (NIRVANA) scheme [8,9] developed by Leonard and SMART (Sharp and Monotonic Algorithm for Realistic Transport), developed by Gaskell and Lau [10], have also gained wide popularity.

In a parallel development, the FCT algorithm has been applied to the Taylor–Galerkin framework to resolve sharp profiles [11–14]. The other approach for constructing oscillation-free schemes is to apply a global positivity principle to numerical analyses which underlie the explicit scheme [15,16]. This boundedness principle demands that coefficients at (i,j), and (m,n) $a_{ij}\phi_{ij} = \Sigma_{m,n}\, a_{mn}\phi_{mn}$ (where m,n are surrounding nodes of i and j, respectively) be positive. Such a sufficient (but not necessary) condition for the discrete solution ensures that ϕ_{ij} is simply a weighted sum of the neighboring values of ϕ_{mn}, thus prohibiting the occurrence of new extrema and enhancing the stability of the explicit scheme. While this principle is straightforward in theory and is easy to implement for existing computer codes, its scope of application is limited to explicit schemes. Filtering techniques that are applicable to finite element analyses involving solutions of simultaneous algebraic equations must, thus, be devised. To avoid erroneous oscillations near jumps, we have modified the test functions defined in the Streamline Upwind Petrov–Galerkin (SUPG) [17] model by means of nonlinear addition [6]. This added stiffness matrix ensures satisfication of either the total variational diminishing property [1] or the maximum principle [18–21]. Exploiting this principle yields a monotonic solution profile. Instead of modifying the test functions, Rice and Schnipke [16] and Hill and Baskharone [22] took a different approach in an attempt to achieve the same goal. Integral terms involving convection terms are evaluated along the local streamline, thus providing monotonic solutions. Readers are referred to other advection–diffusion schemes in [23–25] which were reported to be able to resolve high gradient solutions in the domain of two dimensions.

Recently, the work of Ahue and Telias [20], who used an exponential biased test function to yield an M-matrix, has prompted us to construct a biased weighting function in favor of field variables at the upstream side. Guided by this mathematically rigorous theory, we have successfully captured sharp gradients or discontinuities in the flow [26,27]. The purpose of our continuing research effort is to refine the proposed scheme. Performance is improved in the following direction. In smooth regions, a high-order upwind solution is pursued. In regions where sharp layers or discontinuities are present, a monotonic solution is effectively computed by locally stretching the mesh so that the cell Reynolds number falls into the shaded region shown in Fig. 4. Grid adaption is the other main concern of the present analysis.

We begin by describing in Section 2 the target problem, known as the convection–diffusion equation. We bring the monotonicity-preserving property into the Petrov–Galerkin framework. Bearing in mind that the simulation quality is measured on the basis of both solution accuracy and stability, we have carried out fundamental studies and discussed them here in detail. In order to validate the proposed flux discretization scheme, we will present the closed-form solution for the scalar transport equation defined in a square. Attention is directed to assessing scheme performance.

2. Multi-dimensional flux discretization scheme

2.1. Model equation and discretization method

The working equation which will be considered is the scalar transport equation:

$$u\Phi_x + v\Phi_y = \mu(\Phi_{xx} + \Phi_{yy}). \tag{1}$$

We consider in this study a simple flow, as given by $\vec{u} = (u,v)$, where u and v are two constants. This simplification avoids linearizations on equation nonlinearities. For simplicity, this paper will be further restricted to a constant diffusion coefficient μ in a simply-connected domain D. For the elliptic differential equation given in (1) to be well-posed, it is required to prescribe boundary conditions at the entire boundary of the physical domain D. Depending on the relative importance of convection and diffusion effects, as measured by the maximum values of $Pe_x = (u\,\Delta x)/\mu$ and $Pe_y = (v\,\Delta y)/\mu$, different classes of upwinding schemes are chosen for computational reasons. Here, Δx and Δy denote mesh sizes along the x and y directions, respectively.

Finite element solutions, $\hat{\Phi}$, to the convection dominant transport equation are obtained by demanding that $R = u\hat{\Phi}_x + v\hat{\Phi}_y - \mu(\hat{\Phi}_{xx} + \hat{\Phi}_{yy})$ be orthogonal to the weighting function. Solutions thus obtained can be viewed as a search for the weak solutions to Eq. (1). In the Petrov–Galerkin framework, we demand that the test space, W_i, be different from the trial space N_i. Substitution of 4-node isoparametric bilinear basis functions, $\hat{\Phi} = \Sigma_{i=1}^{4} N_i(\xi,\eta)\Phi_i$, into the weighted residuals statement leads to a matrix equation at the element level. Upon assemblage of finite elements, the global coefficient matrix is formed. There remains selection of test functions to close the algebraic system. How the weighting functions are constructed is of pivotal importance and warrants further discussion.

2.2. Construction of test space

One obstacle to finding satisfactory prediction of the field variable governed by (1) is the presence of first derivative terms. For problems involving multiple dimensions and encountering high Peclet numbers, it is particularly important to model convective fluxes. In this regard, attention will be directed towards circumventing notorious difficulties arising from direction-dependent fluxes. The quality of the upwind scheme can be judged from many aspects. It is crucial that numerical fluxes remain conserved in the course of conducting spatial derivatives (conservativeness). Prediction of a problem of convection-dominated type requires suppression of oscillatory solutions arising from the approximation of convective terms (convective stability). In the development of an advection–diffusion scheme for fluid flows which has potential for use in a wide range of scientific application, it is required that oscillations are by no means allowed to appear even in the vicinity of discontinuities (monotonicity). Petrov–Galerkin finite element models suffice to provide schemes having the first two properties. Whether or not the boundedness property can be rendered is closely related to the coefficient matrix. According to the work of Ahue and Telias [20], a matrix of the diagonal dominant type is a key to permitting bounded solutions. To achieve this sufficient condition for arriving at bounded solutions, we have to bias the weighting function in favor of the upwind side. In [26,27], Sheu et al. constructed an exponential weighting function which has the property of yielding an M-matrix [18–20]. Promising application of this upwind finite element model is rooted in the fact that it is well suited for both incompressible Navier–Stokes equations and a pure advection equation [26,27]. One disadvantage inherent in this model is that the use of exponential functions for finite element integration can produce prohibitively high computational costs. This deficiency motivates us to refine this model with a view to improving efficiency by constructing a new test space which is spanned by Legendre polynomials [28]. The reason for choosing this class of orthogonal functions is two-fold. First, exploiting the fact that any exponential function can be spanned by a series of Legendre polynomials, we are led to construct a monotone stiffness matrix. Second, the orthogonal property inherent in this class of polynomials considerably facilitates numerical integration. The justification for using the following weighting functions has been presented in [28]:

$$\begin{aligned} W_i &= D_i W_\xi(\xi) W_\eta(\eta) \\ &= D_i \sum_{n=0}^{\infty} d_{\xi_n} P_n(\xi) \sum_{n=0}^{\infty} d_{\eta_n} P_n(\eta) \end{aligned} \tag{2}$$

where

$$\begin{aligned} D_i &= \frac{1}{4} \exp\left(\frac{u h_\xi \xi_i}{2\mu}\right) \exp\left(\frac{v h_\eta \eta_i}{2\mu}\right), \\ W_\xi(\xi) &= (1 + \xi_i \xi) \exp\left(-\frac{u h_\xi \xi}{2\mu}\right), \\ W_\eta(\eta) &= (1 + \eta_i \eta) \exp\left(-\frac{v h_\eta \eta}{2\mu}\right), \\ d_{\xi_n} &= \frac{2n+1}{2} \int_{-1}^{1} W_\xi(t) P_n(t)\, \mathrm{d}t, \\ d_{\eta_n} &= \frac{2n+1}{2} \int_{-1}^{1} W_\eta(t) P_n(t)\, \mathrm{d}t. \end{aligned}$$

In Eq. (2), h_ξ and h_η denote grid sizes. Eq. (2) involves the Legendre polynomials $P_0(t) = 1$ and $P_1(t) = t$. For clarity, we have plotted the piecewise weighting function in a block of four bilinear elements having a common reference node (i,j). As Fig. 1 indicates, the stability enhancement is directly attributable to the biased part of the Legendre polynomials defined in Eq. (2). For this upwind model to be computationally competitive with other classes of upwind schemes, we take advantage of the orthogonal property inherent in the space of Legendre polynomials:

$$\int_{-1}^{+1} P_i(t) P_j(t)\, \mathrm{d}t = \frac{2}{2i+1} \delta_{ij} \quad (i \text{ is dummy index}). \tag{3}$$

With knowledge, then, of this mathematically appealing integral identity, an unacceptable increase in CPU time can be avoided. It is for this reason that we are prompted to rewrite bilinear shape functions $N_i(\xi, \eta)$ in terms of Legendre polynomials as follows:

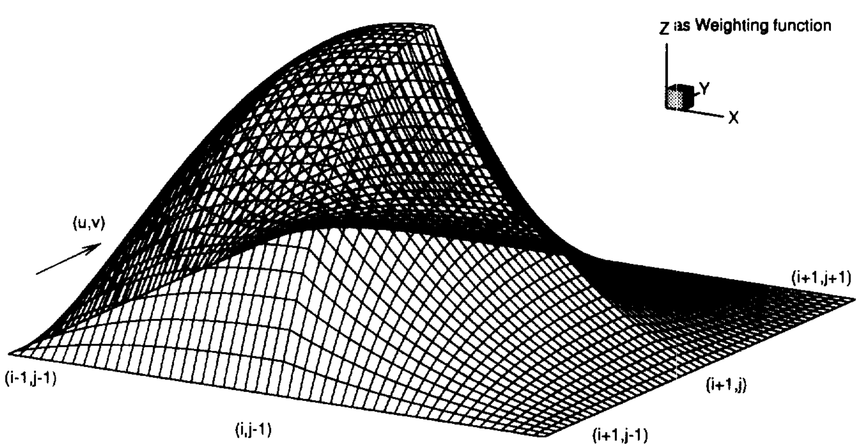

Fig. 1. Piecewise weighting function in a block of four bilinear elements.

$$N_i(\xi,\eta) = \frac{1}{4}(1 + \xi_i \xi)(1 + \eta_i \eta),$$
$$= \frac{1}{4}[P_0(\xi) + \xi_i P_1(\xi)]\,[P_0(\eta) + \eta_i P_1(\eta)]. \tag{4}$$

Before proceeding to the fundamental study, it is worthwhile to address the advantage of using Legendre polynomials. As shown in our previous paper [28], using this class of Legendre polynomials amounts to producing the same matrix equation by employing our previously developed exponential weighting functions [26,27]. Much fewer Gaussian integration points are, however, needed. This explains why CPU time is considerably reduced without any loss of solution accuracy. For a detailed proof of the mathematic equivalence between two upwind finite element models, the reader is referred to the work of Sheu et al. [28].

3. Fundamental studies

3.1. Modified equation analysis

There are several areas which require detailed investigation before a newly developed discretization scheme can come into widespread use for industrial flows. Typical of them is modified equation analysis. This fundamental analysis gives insight into the order-of-accuracy issue in finite element approximation and assures that a uniformly consistent property can be obtained. Following the standard procedures of Warming and Hyett [29], we can derive the following modified equation for the working equation given by (1):

$$u\,\Phi_x + v\,\Phi_y - \mu\,(\Phi_{xx} + \Phi_{yy}) = T, \tag{5}$$

where

$$T = c_1\Phi_{xx} + c_2\Phi_{xy} + c_3\Phi_{yy} + d_1\Phi_{xxx} + d_2\Phi_{yyy} + d_3\Phi_{xxy} + d_4\Phi_{xyy}$$
$$e_1\Phi_{xxxx} + e_2\Phi_{xxxy} + e_3\Phi_{xxyy} + e_4\Phi_{xyyy} + e_5\Phi_{yyyy} + \cdots \tag{6}$$

Algebraic complications preclude expression of the above coefficient terms in functional form. To reveal how the discretization error, T, varies with the spatial interval, we have plotted discretization errors logarithmatically against grid sizes, from which the rates of convergence for derivative terms in T can be obtained. As Fig. 2 reveals, the rates of convergence for Φ_{xxxy} and Φ_{xyyy} are $\mathcal{O}(h^4)$ while those for Φ_{xy}, Φ_{xxx}, Φ_{yyy}, Φ_{xxy}, Φ_{xyy}, Φ_{xxxx}, Φ_{yyyy} and Φ_{xxyy} are in the vicinity of $\mathcal{O}(h^2)$. As to the leading terms, Φ_{xx} and Φ_{yy}, their errors are reduced by a convergence rate of $\mathcal{O}(h^2)$. In light of the results of modified equation analysis, the finite element discretization method presented here clearly possesses the consistency property with second-order accuracy. The overall rate of convergence is problem-dependent. In the case of $(u, v) = (1/(x + 1/2),\ 1(y + 1/2))$ and $\mu = 1$, the rate of convergence can be clearly seen from Table 1, which plots the $\log(\mathrm{err}_1/\mathrm{err}_2)$ against $\log(M_1/M_2)$. Here, $\mathrm{err}_i (i = 1,2)$ denotes L_2-norms of errors computed at two continuously refined grids, $(M_1 + 1) \times (M_1 + 1)$ and $(M_2 + 1) \times (M_2 + 1)$.

3.2. Fundamental studies on solution monotonicity

The present section focuses on numerical suppression of erroneous oscillations. These oscillations, arising from the third-order dispersion error shown in the modified equation, are amplified in regions where sharp gradients appear. Within the finite element framework, we follow the rule of Ahue and Telias [20] to achieve the goal of obviating the extraneous extreme in the solution. According to their study, the presence of a monotonic transport profile is only the result of the monotone stiffness matrix for the advection–diffusion equation. By definition, when $\boldsymbol{M}\Phi \geqslant 0$ holds for any vector Φ, the components of Φ are also positive. Under these circumstances, a matrix $\boldsymbol{M}$ is termed monotonic. The sufficient (but not necessary) condition for solutions to be monotonic is that the stiffness matrix formed is a real and irreducible diagonally dominant matrix where off-diagonal entries are non-negative [18–21]. At this point, it is instructive to examine whether the upwind scheme formulated on the basis of Legendre-polynomial finite element spaces can be applied to yield an

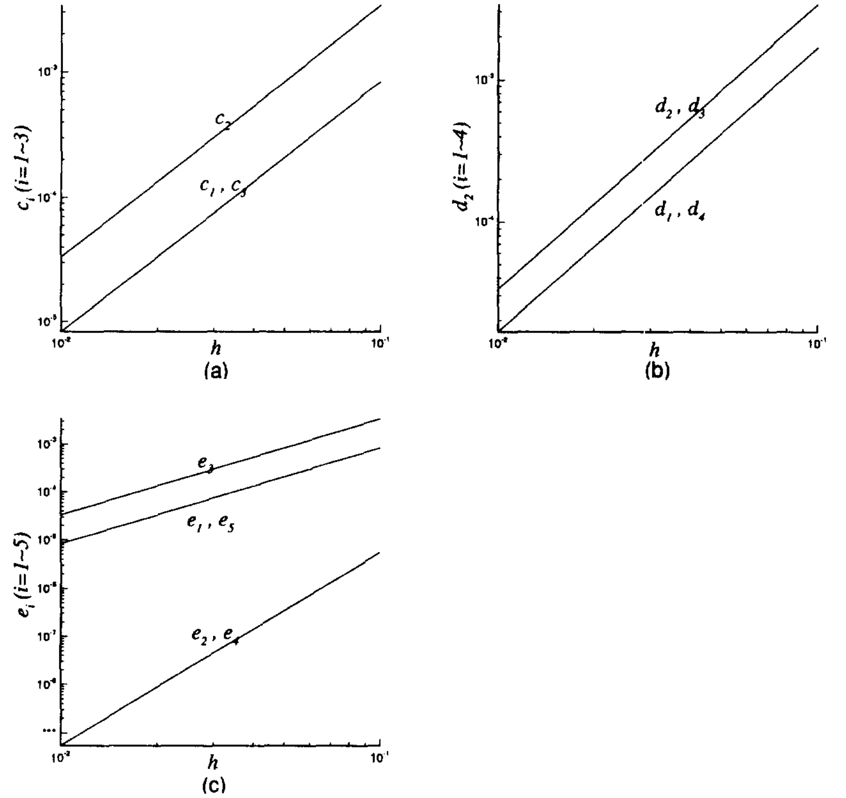

Fig. 2. Rates of convergence: (a) Φ_{xx}, Φ_{xy}, Φ_{yy}; (b) Φ_{xxx}, Φ_{xxy}, Φ_{xyy}, Φ_{yyy}; (c) Φ_{xxxx}, Φ_{xxxy}, Φ_{xxyy}, Φ_{xyyy}, Φ_{yyyy}.

Table 1
Rate of convergence for the test case defined in Section 3.2 using the proposed discretized advection-diffusion scheme.

Element	L_2-norm	Convergence rate
5×5	3.2614×10^{-3}	
		3.36
10×10	3.1738×10^{-4}	
		3.19
20×20	3.4681×10^{-5}	
		3.29
40×40	3.5297×10^{-6}	

unconditionally monotonic solution. To this end, we derive the discrete finite element equation from four bilinear elements shown in Fig. 3. Like the finite difference setting at the point 'j', the discrete equation, showing the implicit relation with its eight surrounding nodal values, is represented symbolically as $\Sigma_1^9\, a_i \Phi_i = 0$. Although the effort required to derive mathematical expressions of $a_i = a_i(\mathrm{Pe}_x, \mathrm{Pe}_y, h)$ is considerable, it is useful to decide under what conditions the coefficient matrix can be classified as being irreducible diagonally dominant. To clearly demonstrate that a monotonic solution can be obtained from the matrix equation thus derived, we have calculated the coefficients of a_i. By varying the values of Pe_x against Pe_y, the shaded area in Fig. 4 is regarded as a stable domain. By definition, we mean that within a stable regime there is an upper limit on the allowable Peclet number, above which the finite element solution deteriorates. This implies that, for the problem considered and the domain discretized, the underlying discrete maximum principle allows us to obtain a monotonic solution. While the choice of test function tends to yield an M-matrix equation, the rather restricted constraint condition has limited practioners to a small grid size. The mesh is continuously enriched with nodes in the entire domain which may result in increasingly smaller Peclet numbers and may help to suppress oscillations. The refinement, however, produces prohibitively high computational costs in computing monotonic

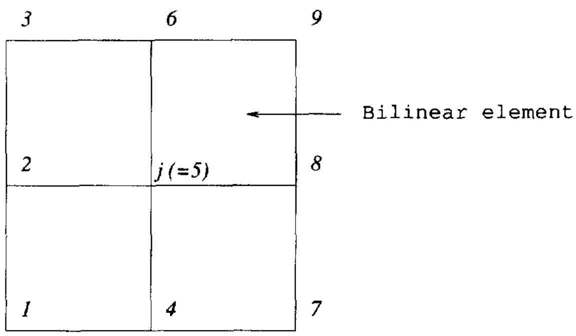

Fig. 3. Illustration of the relation among points of the discretized equation in a pack of four bilinear elements.

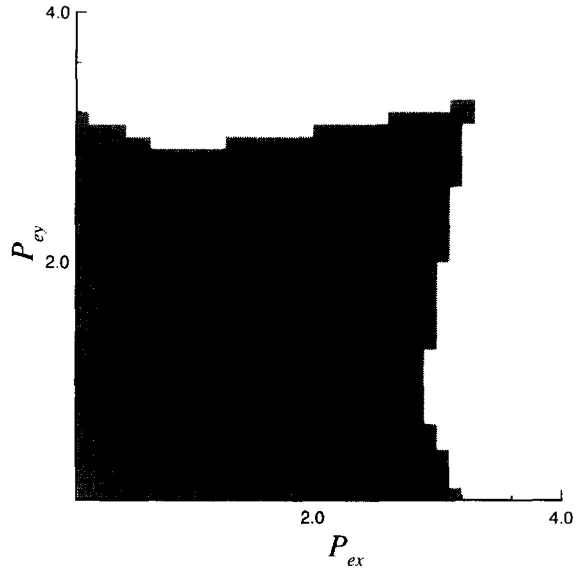

Fig. 4. Stable region.

solutions. This presents computational difficulties in extending the theoretically appealing model to a wider scope of applications. Consideration will be given later to circumventing this difficulty. It is worthwhile to note that when this analysis is reduced to one dimension, the discretization equation turns out to be exactly the localized adjoint method of Celia [30].

4. *h*-adaptive finite element solution algorithm

As noted earlier, the scope of the proposed monotonic flux discretization method so far used is limited to Peclet numbers falling into the shaded area in Fig. 4. This restricted constraint condition precludes extension of the proposed model to a wider range of applications. We are, thus, prompted to reduce the computational cost and disk storage demand for a high resolution numerical simulation. There are several effective ways to satisfy this constraint requirement. The present paper conquers this difficulty by making modifications to the conventional structured-type finite element formulation. The underlying idea is that, in a smooth region, the Legendre-polynomial finite element solution is desired while in regions containing a steep gradient, the aim is to adaptively regrid the mesh in an attempt to monotonically capture the local jump in the solution.

This suggests use of an h-adaptive method since grid sizes can be rationally chosen. The goal behind grid adaption is to increase the number of points only in high gradient regions, thus increasing the overall solution quality at reasonable cost. The guideline for deciding on which cells to divide and undivide follows the discrete maximum principle discussed in Section 3.2. Assessment of grid refinement depends on, among other factors, complications in data structure, bookkeeping of remeshed nodes, and the treatment of constrained nodes. A recent comprehensive survey of various data structures for implementing h-adaptive finite element methods has been compiled by Demkowicz and Oden [31]. For the correct treatment of constrained nodes, refer to the papers of Devloo et al. [32], of Demkowicz et al. [33] for two-dimensional problems, to the work of Huang et al. [34,35] for axisymmetric problems, and to Devloo [36] for three-dimensional problems. It has to be pointed out that the data structures designed by Devloo et al. [32,36], although not very efficient, are quite straightforward and have been successfully applied to a family of adaptive explicit/implicit Taylor–Galerkin finite element methods to solve a wide range of two-dimensional [37] and axisymmetric [34,35,38] flow problems.

According to Demkowicz and Oden [31], a node is said to be regular if it is a corner vertex of each of neighboring elements, and a mesh is said to be regular if all its nodes are regular. All other nodes are classified as irregular (or hanging nodes). A typical situation for hanging nodes where the 1-irregular rule [31] is applied is shown in Fig. 5. This type of hanging node is encountered along the side of inter-elements with different levels

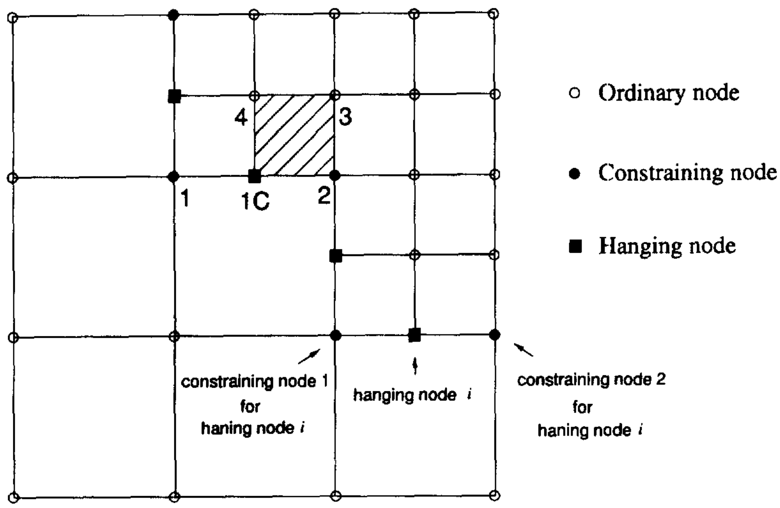

Fig. 5. Illustration of the hanging node and constraining nodes.

of refinement. Within the finite element framework, numerical solutions at these irregular nodes cannot be considered as the degrees of the freedom for a problem. Rather, they are constrained by the solutions of regular nodes on the constraining side. The constrained relations are actually determined by the mesh refinement strategy. Successful application of the h-refinement technique in finite element analysis depends greatly on the correct treatment of hanging nodes.

In the remainder of this section, we will present the method for correct treatment of hanging nodes. If bisecting an element is adopted as the strategy for mesh refinement, then the hanging node is located at the mid-point of a side of the coarser mesh. Since the numerical solution in an element is approximated by the bilinear shape function, the solution on the hanging node 1C of the shaded element shown in Fig. 5 is constrained by the following relation:

$$u_{1C} = \frac{1}{2}(u_1 + u_2). \tag{7}$$

This constrained relation eliminates the degree of freedom associated with node 1C and results in a modification of both the element mass matrix, $\boldsymbol{M}^e$, and the global mass matrix, $\boldsymbol{M}$. The modified element mass matrix can be simply expressed as

$$\tilde{\boldsymbol{M}}^e = \boldsymbol{P}\boldsymbol{M}^e\boldsymbol{P}^{\mathrm{T}}, \tag{8}$$

where $\boldsymbol{M}^e$, $\tilde{\boldsymbol{M}}^e$ represent the original and modified element mass matrices, respectively, and $\boldsymbol{P}$ is the permutation matrix

$$\boldsymbol{P} = \begin{bmatrix} \frac{1}{2} & 0 & 0 & 0 \\ \frac{1}{2} & 1 & 0 & 0 \\ 0 & 0 & 1 & 0 \\ 0 & 0 & 0 & 1 \end{bmatrix}. \tag{9}$$

Although the modification procedure (8) is implemented at the element level, it complicates the coding and may cause some problems in vectorizing the code; therefore, it is not adopted in our code. Instead, the overall computation efficiency can be improved by modifying the global mass matrix, $\boldsymbol{M}$, directly. Following the approach of Demkowicz et al. [33], the entries of the rows and columns of the global mass matrix corresponding to the hanging node will be eliminated and distributed to the rows and columns of the two corresponding constraining nodes according to

$$M_{k_r(i),\hat{j}} = M_{k_r(i),\hat{j}} + \frac{1}{2}M_{i,\hat{j}},$$

$$M_{\hat{i},l_s(j)} = M_{\hat{i},l_s(j)} + \frac{1}{2} M_{\hat{i},j}, \tag{10}$$

$$M_{k_r(i),l_s(j)} = M_{k_r(i),l_s(j)} + \frac{1}{4} M_{i,j},$$

where i, j are the indices of the rows and columns of a hanging node in an algebraic equation, $k_r(i)$, $l_s(j)$ are the indices of the rows and columns of the corresponding constraining node, r, $s = 1$, or 2 for the two constraining nodes, and $\hat{i}$, $\hat{j}$ are indices of rows and columns other than those of the hanging node. The right-hand side vector $\boldsymbol{b}$ will be changed to

$$b_{k_r(i)} = b_{k_r(i)} + \frac{1}{2} b_i, \tag{11}$$

and row i and column j will be eliminated, so we will obtain a value of u_i from Eq. (7) instead of obtaining it directly from the algebraic equation.

5. Numerical studies

The test cases chosen for validation and assessment of the newly developed upwind finite element model and the h-refinement technique are: (i) a boundary-layer type test problem; and (ii) a skew advection–diffusion problem. Common to both tests are the geometric simplicity and the mesh regularity. These features assure of the reliability of computing metric tensors.

5.1. Ananalytic study of a boundary-layer type problem

The first problem we will deal with is that of a non-smoothly varying transport problem. This problem is configured in Fig. 6. Subject to boundary data prescribed on the entire boundary, the advection–diffusion equation is amenable to boundary-layer type analytic solution:

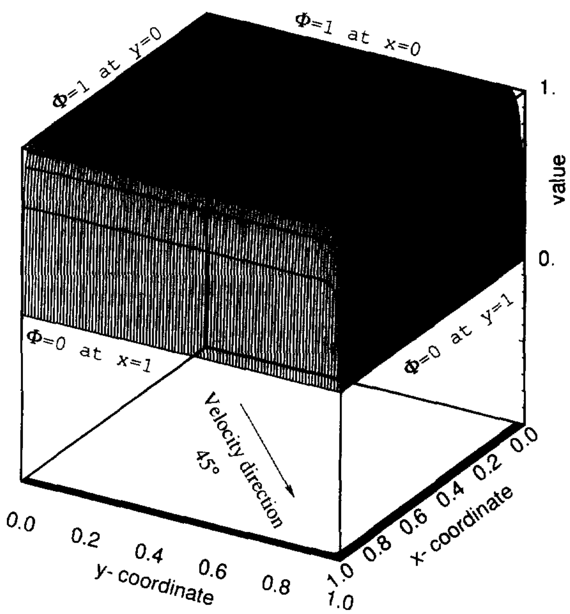

Fig. 6. Configuration of the problem defined in Section 5.1.

$$\Phi(x,y) = \frac{\left[1-\exp\left(x-1\right)\frac{u}{\mu}\right)\Big]\left[1-\exp\left((y-1)\frac{u}{\mu}\right)\right]}{\left[1-\exp\left(-\frac{u}{\mu}\right)\right]\left[1-\exp\left(-\frac{u}{\mu}\right)\right]}. \tag{12}$$

This problem is chosen to verify the applicability of the finite element model developed here to problems involving a boundary layer profile. Finite element solutions are sought at grids, starting from a coarse regular grid, as shown in Fig. 7(a), and moving on to adaptively refined grid levels, as given in Fig. 7(b–d). Prediction errors for the case considered ($\mu = 10^{-2}$) are measured in their L_2-norm forms, from which we can assess the effectiveness of the grid adaptivity. Besides enhancement of solution monotonicity, solution accuracy also

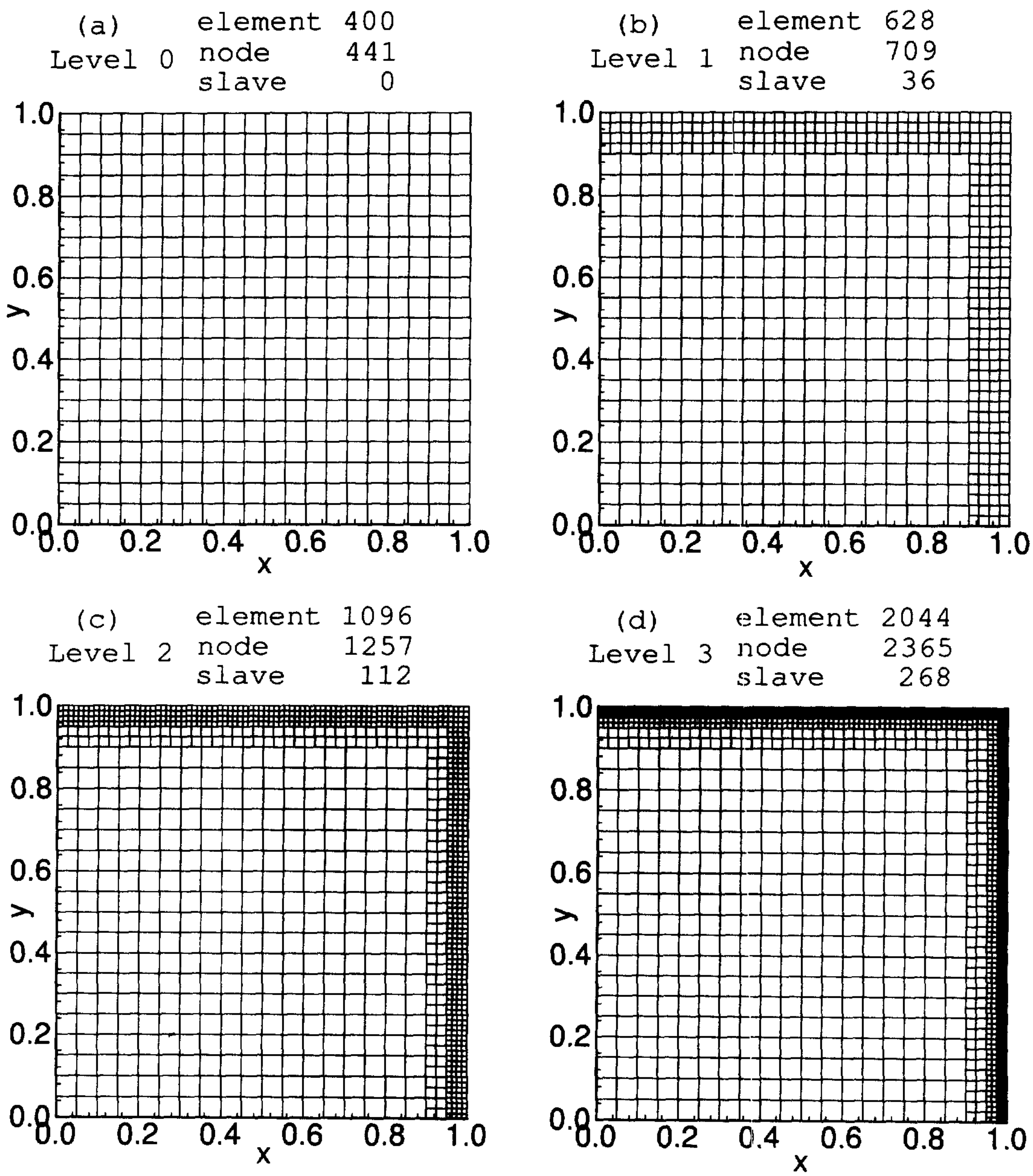

Fig. 7. Meshes of the problem defined in Section 5.1.

Table 2
L_2-norm comparison of problem defined in Section 5.1

Adaptive level	Node number	L_2-norm	Compared regular node number	L_2-norm
0	441	1.614×10^{-2}	441	1.614×10^{-2}
1	709	1.447×10^{-2}	729	1.486×10^{-2}
2	1257	6.696×10^{-3}	1296	1.123×10^{-2}
3	2365	4.361×10^{-3}	2401	7.089×10^{-3}

improves with an increase of the number of adaptive levels. Shown in Table 2, for comparison purposes, are the computed L_2-error norms for calculations which involve roughly the same number of regular mesh points. According to Fig. 8, which depicts the computed advective profile against continuously refined unstructured grids, the present finite element formulation has the ability to get around difficulties associated with a rapid change of solution in the flow.

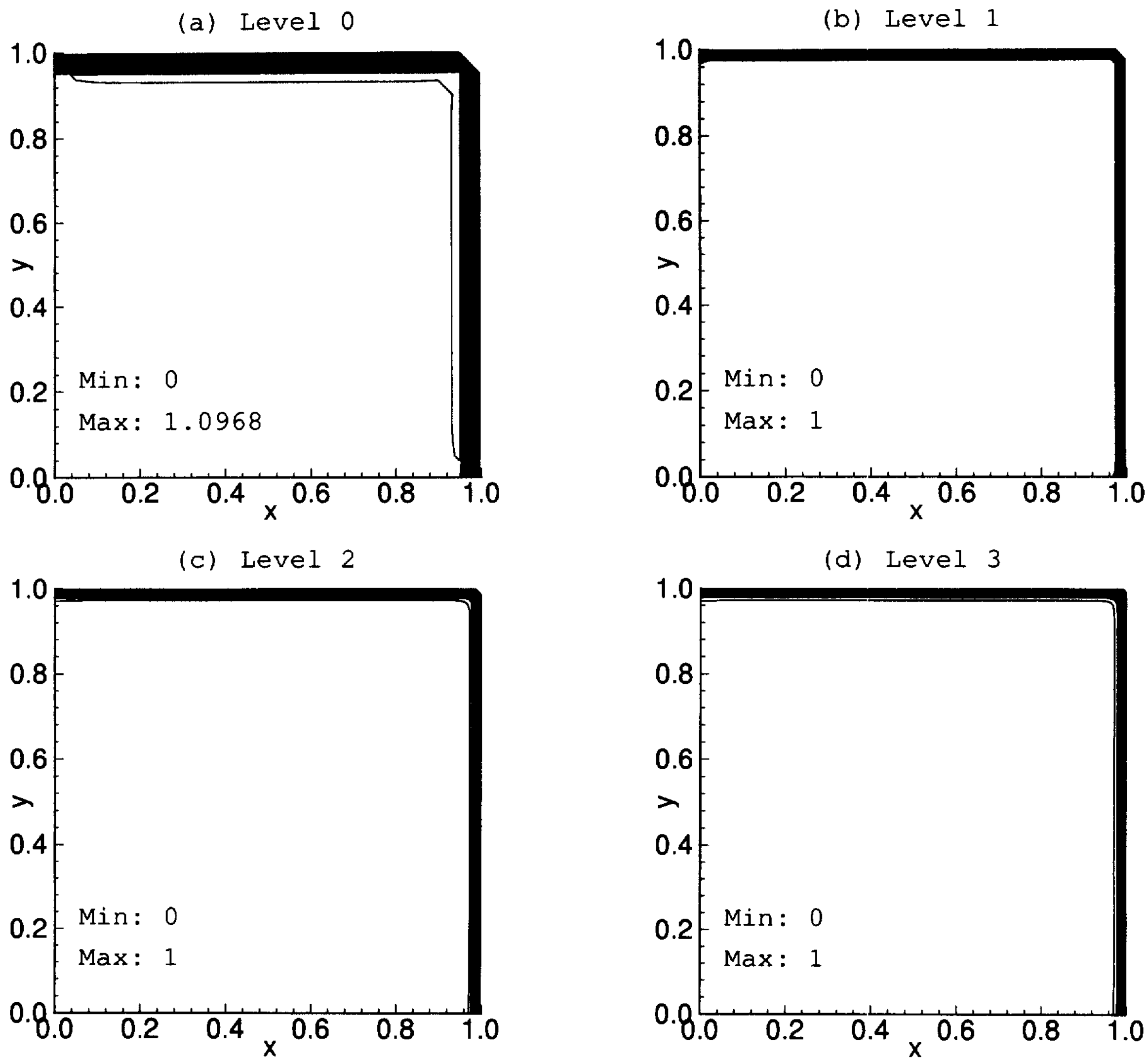

Fig. 8. Solutions of the problem defined in Section 5.1.

5.2. Skew advection-diffusion problem

An even harder problem follows. This problem, known as the skewed flow transport problem, is featured by an internal layer and is regarded as a worst case scenario for any upwinding method [39]. Within a square cavity of unit length, a tilted line passing through a corner point at (0,0), making a slope of $m = \tan^{-1} v/u$, divides the cavity into two subdomains. In the whole domain, the magnitude of velocity remains unchanged while $q = \sqrt{u^2 + v^2} = 1$. Subject to the boundary condition for the working variable given in Fig. 9, there is a sharp change in the transport variable across the dividing line.

The goal of using this case is to assess the merits and the drawbacks of the proposed upwinding technique. We consider in a unit square that there is a uniform flow parallel to a dividing line. As Fig. 10 indicates, the physical domain is covered by a grid of 20×20 boxes with $\Delta x = \Delta y$. Different diffusivities are considered, which result in different degrees of advection dominance. Given the value of diffusivity 1.67×10^{-2}, the cell Peclet number

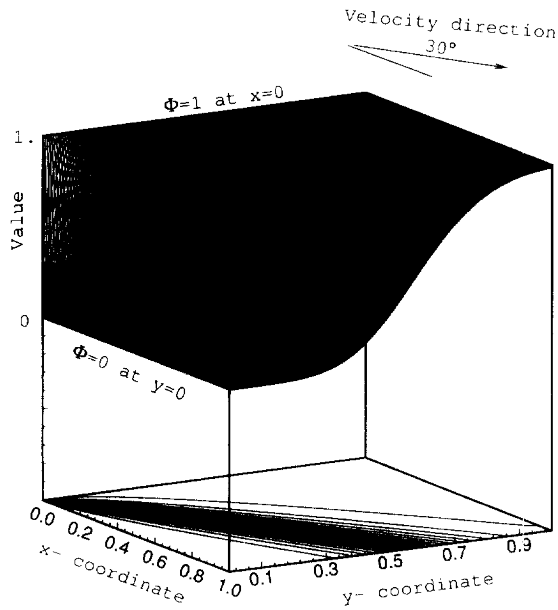

Fig. 9. Configuration of the problem defined in Section 5.2.

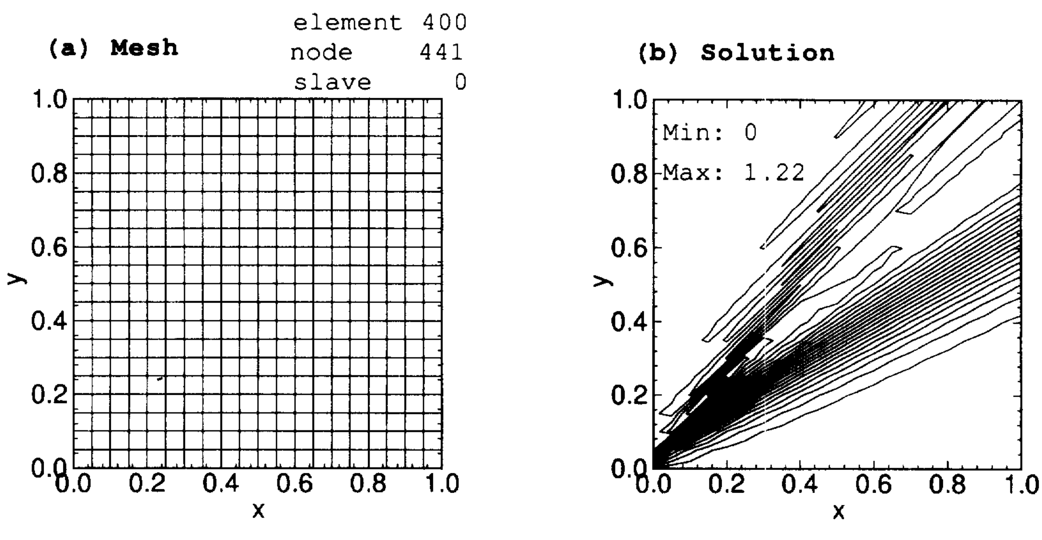

Fig. 10. The mesh and solution of problem defined in Section 5.2 with uniform mesh.

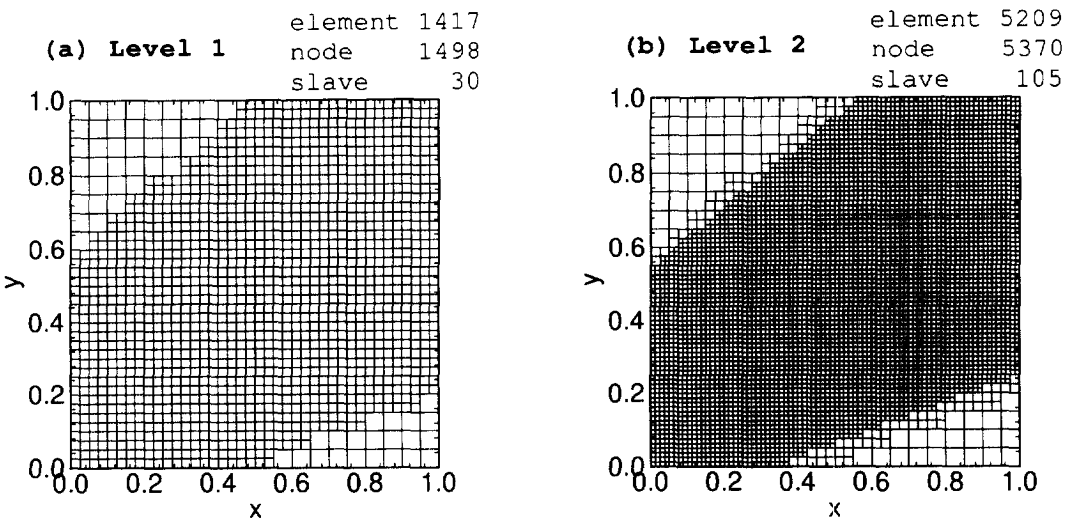

Fig. 11. The meshes of the h-adaptive technique of the problem defined in Section 5.2.

approaches 3 and falls into the monotonic regime. Oscillation-free finite element solutions, as shown in Fig. 10, are computed in regions not only close to, but also away from the dividing line. This reveals that non-physical spatial oscillations are never exhibited under these circumstances. On increasing the Peclet numbers or decreasing the diffusivity to $\mu = 10^{-2}$, there is gross oscillation in the solution of the field variable Φ, which implies that this method is inapplicable to problems involving steep gradients. There may be two ways to avoid these wiggles. One may keep reducing the mesh size until the corresponding Peclet number falls into the monotonic region defined in Fig. 4. This, however, involves considerable computational expense. This drawback makes practical computation infeasible. We, thus, turn to refining the solution algorithm by using an h-refinement technique.

According to Fig. 11, use of an h-adaptive refinement technique makes it possible to obtain monotonic solutions in a domain discretized by many fewer elements. Since this problem is not amenable to analytic solution, a fine grid solution of resolution 160×160 is taken as a basis for comparison. As compared with finite element solutions computed for much denser grids, as shown in Fig. 11, monotonic solutions are also adaptively computable in a domain which has been discretized in an unstructured manner, as shown in Fig. 12. This clearly demonstrates the algorithmic superiority of resolving internal layers. We have also tabulated the computed

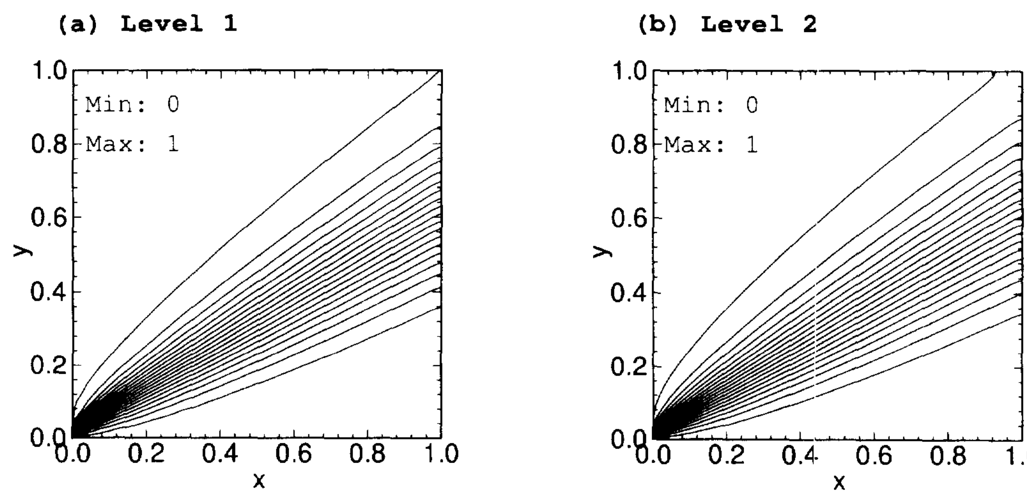

Fig. 12. The solutions of the h-adaptive technique of the problem defined in Section 5.2.

Table 3
L_2-norm comparison of problem defined in Section 5.2

Adaptive level	Node number	L_2-norm
0	441	8.222×10^{-2}
1	1498	3.224×10^{-2}
2	5370	2.966×10^{-2}

L_2-error norms with reference to a solution computed on the basis of 160×160 uniform grids, as shown in Table 3.

6. Conclusions

Legendre polynomials have been selected for use in constructing the basis and test spaces. There are several reasons for this innovative choice, foremost of which is that use of test functions spanned by Legendre polynomials of sufficiently lower order tends to yield a monotone stiffness matrix. Secondly, the orthogonal property inherent among Legendre polynomials facilitates numerical integration in that many fewer Gaussian integration points are needed to render exact integration. An in-depth fundamental study to the discretization scheme has provided insight into order-of-accuracy estimation in finite element approximation. With a decrease of the grid size, the local error is reduced by an order of $\mathcal{O}(h^2)$, confirming, thus, the consistency of the discretization scheme. We use the discrete maximum principle as our guide in studying the stability of the scheme. Through this study, we have learned that the stiffness matrix is not unconditionally classified as an M-matrix. If Peclet numbers fall below the critical Peclet number, then the discrete system can by no means be classified as an M-matrix; thus, monotonic solutions cannot possibly be rendered. While monotone solutions can be obtained by continuously refining the mesh, the computational cost will be prohibitively high due to the restriction imposed on the grid size. Guided by the underlying discrete maximum principle, we are able to determine which grid warrants further discretization. Use of an h-adaptive mesh in the present upwind finite element analysis makes highly convection-dominated and locally graded computation possible on conventional workstations without the need to use many elements to avoid oscillations near steep gradients.

Acknowledgments

The authors would like to thank the Computer Center of National Taiwan University and the National Center for High-performance Computing (NCHC) for providing CRAY J916 and IBM RS/6000-590 computers, which made this study possible. Research support by the National Science Council of Republic of China under Grant NSC84-2212-E-002-060 is also gratefully acknowledged.

References

[1] A. Harten, High resolution schemes for hyperbolic conservation law, J. Comput. Phys. 49 (1993) 357–393.

[2] J.P. Boris and D.L. Book, Flux corrected transport I SHASTA, A fluid transport algorithm that works, J.Comput. Phys., 11 (1973) 38–69.

[3] S.T. Zalesak, Fully multidimensional flux-corrected transport algorithm for fluids, J. Comput. Phys. 31 (1979) 335–362.

[4] M. Chapman, FARM-nonlinear damping algorithm for the continuity equation, J. Comput. Phys. 44 (1981) 84–103.

[5] T.W.H. Sheu, S.M. Lee, K.O. Yang and B.J.Y. Chiou, A non-oscillating solution technique for skew and QUICK-family schemes, Comput. Mech. 8 (1991) 365–382.

[6] T.W.H. Sheu, P.G.Y. Huang and M.M.T. Wang, A discontinuity SUPG formulation using quadratic elements, in: Ch. Hirsch, ed., Proceedings of the First European Computational Fluid Dynamics Conference, Vol. 1 (Elsevier, 1992) 125–129.

[7] B.P. Leonard, Simple high-accuracy resolution program of convective modeling of discontinuity, Int. J. Numer. Methods Fluids 8 (1988) 1291–1318.

[8] B.P. Leonard, A.P. Lock and M.K. MacVean, The NIRVANA scheme applied to one-dimensional advection, Int. J. Numer. Methods Heat Fluid Flow 5 (1995) 341–377.
[9] B.P. Leonard, A.P. Lock and M.K. MacVean, Extend numerical integration for genuinely multidimensional advective transport insuring conservation, Numerical Methods in Laminar and Turbulent Flow '95, IX (Part 1) (1995) 1–21.
[10] P.H. Gaskell and A.K.C. Lau, Curvature compensated convective transport: SMART a new boundedness preserving transport algorithm, Int. J. Numer. Methods Fluids 8 (1988) 617–641.
[11] R. Löhner, K. Morgan, J. Peraire and M. Vahdati, Finite element flux-corrected transport (FEM-FCT) for the Euler and Navier-Stokes equations, Int. J. Numer. Methods Fluids 7 (1987) 1093–1109.
[12] T.W.H. Sheu and C.C. Fang, A flux corrected transport finite element method for multi-dimensional gas dynamics, Proceedings of the Second European Computational Fluid Dynamics Conference (ECCOMAS), (Elsevier, 1994) 170–175.
[13] T.W.H. Sheu and C.C. Fang, A high resolution finite element analysis for nonlinear acoustic wave propagation, J. Comput. Acoust. 2(1) (1994) 29–51.
[14] T.W.H. Sheu and C.C. Fang, A numerical study of nonlinear propagation of disturbances in two-dimensions, J. Comput. Acoust. 4(3) (1996) 291–319.
[15] S. Spekreijse, Multigrid solution of monotone second-order discretizations of hyperbolic conservation laws, Math. Comput. 49 (1987) 135–155.
[16] J.G. Rice and R.J. Schnipke, A monotone streamline upwind finite element methods for convection-dominated flows, Comput. Methods Appl. Mech. Engrg. 47 (1984) 313–327.
[17] T.J.R. Hughes and A. Brooks, A multi-dimensional upwind scheme with no crosswind diffusion, in: T.J.R. Hughes, ed., Finite Element Methods for Convection Dominated Flows, AMD 34 (ASME, New York, 1979) 19–35.
[18] T. Meis and U. Marcowitz, Numerical solution of partial differential equations, Applied Mathematical Science, Vol. 32 (Springer-Verlag, 1981).
[19] T. Ikeda, Maximal principle infinite element models for convection-diffusion phenomena, in: Lecture Notes in Numerical and Applied Analysis, Vol. 4 (North-Holland, Kinokuniya, Amsterdam, Tokyo, 1983).
[20] M. Ahu and M. Telias, Petrov-Galerkin scheme for the steady state convection diffusion equation, Finite Elements Water Res. (1982) 2/3.
[21] R.S. Varga, Matrix Iterative Analysis (Prentice-Hall, London, 1982)
[22] D.L. Hill and E.A. Baskharone, A monotone streamline upwind method for quadratic finite elements, Int. J. Numer. Methods Fluids 17 (1983) 463–475.
[23] A.C. Galeão and E.G. Dutra do Carmo, A consistent approximate upwind Petrov-Galerkin formulation for convection-dominated problems, Comput. Methods Appl. Mech. Engrg. 68 (1988) 83–95.
[24] H. Deconinck, H. Pailléere, R. Struijs and P.L. Roe, Multidimensional upwind schemes based on fluctuation-splitting for system of conservation laws, J. Comput. Mech. 11 (1993) 323–340.
[25] J.W. Barrett and K.W. Morton, Approximate symmetrization and Petrov-Galerkin methods for diffusion-convection problems, Comput. Methods Appl. Mech. Engrg. 45 (1984) 97–122.
[26] T.W.H. Sheu, M.T. Wang and S.F. Tsai, A Petrov-Galerkin finite element model for analyzing incompressible flows at high Reynolds numbers, Int. J. Comput. Fluid Dyn. 5 (1995) 213–230.
[27] T.W.H. Sheu, S.F. Tsai and M.M.T. Wang, A monotone multidimensional upwind finite element method for advection-diffusion problems, Int. J. Numer. Heat Trans., Part B: Fundamentals 29 (1996) 325–344.
[28] T.W.H. Sheu, S.F.Tsai and M.M.T. Wang, A monotone finite element method with test space of Legendre polynomials, Comput. Methods Appl. Mech. Engrg. 143 (1997) 349–372.
[29] R.F. Warming and B.J. Hyett, The modified equation approach to the stability and accuracy analysis of finite-difference method, J. Comput. Phys. 14 (1974) 159–179.
[30] M.A. Celia and W.G. Cray, Numerical Methods for Differential Equations (Prentice-Hall International Inc., 1992).
[31] L. Demkowicz and J.T. Oden, A Review of Local Refinement Techniques and the Corresponding Data Structures in h-type Adaptive Finite Element Methods, TICOM Report 88-02, The Texas Institute for Computational Mechanics, The University of Texas at Austin, Texas 78712.
[32] P.R. Devloo, J.T. Oden and T. Strouboulis, Implementation of an adaptive refinement technique for the SUPG algorithm, Comput. Methods Appl. Mech. Engrg. 61 (1987) 339–358.
[33] L. Demkowicz, J.T. Oden, W. Rachowicz and O. Hardy, Toward a universal h-p adaptive finite element strategy, Part 1, Constrained approximation and data structure, Comput. Methods Appl. Mech. Engrg. 77 (1989) 79–112.
[34] C.Y. Huang, W.W. Tworzydlo, C. Cullen, Vadaketh, J.M. Bass and J.T. Oden, Adaptive finite element methods for accurate prediction of internal flows in solid rocket booster, Final Report to NASA Marshall Space Flight Center, Contract No. NAS8-37682, The Computational Mechanics Company, Austin, Texas (March 1991).
[35] C.Y. Huang, H.W. Lee and S.J. Wang, Post-processing of a given velocity field—streamlines on adapted unstructured mesh, Proceedings of the 12th National Conference of the CSME, National Chung-Chen University, Chia-Yi, Taiwan, R.O.C. (Nov. 1995).
[36] P.R. Devloo, A three-dimensional adaptive finite element strategy, Comput. Struct. 38 (1991) 121–130.
[37] W.W. Tworzydlo, J.T. Oden and E.A. Thornton, Adaptive implicit/explicit finite element method for compressible viscous flows, Comput. Methods Appl. Mech. Engrg. 95 (1992) 397–440.
[38] W.W. Tworzydlo, C.Y. Huang and J.T. Oden, Adaptive implicit/explicit finite element methods for axisymmetric viscous turbulent flows with moving boundaries, Comput. Methods Appl. Mech. Engrg. 97 (1992) 245–288.
[39] D.F. Griffiths and A.R. Mitchell, Infinite element for convection dominated flows, in: T.J.R. Hughes, ed., AMD 34, (ASME, New York, 1979) 91–104.